Suppression of Sequential Charge Transitions in Ca0.5Bi0.5FeO3 via B-Site Cobalt Substitution

Suppression of Sequential Charge Transitions in $Ca_{0.5}Bi_{0.5}FeO_3$ via B-site Cobalt Doping

Fabio Denis Romero[1,2,*], Peng Xiong[1], Midori Amano Patino[1], Takashi Saito[1], Paula Kayser[3], J. Paul Attfield[3], and Yuichi Shimakawa[1,*]

1. Institute for Chemical Research, Kyoto University, Gokasho, Uji, Kyoto 611-0011, Japan
2. Hakubi Center for Advanced Research, Kyoto University, Yoshida-honmachi, Sakyo-ku, Kyoto 606-8501, Japan
3. Centre for Science at Extreme Conditions and School of Chemistry, The University of Edinburgh, Edinburgh EH9 3JZ, UK

Abstract

The perovskite $Ca_{0.5}Bi_{0.5}FeO_3$ containing unusually high valent $Fe^{3.5+}$ undergoes sequentially charge disproportionation (CD) of the Fe centres and intersite charge transfer (CT) between Bi and Fe. From structural, magnetic, and transport property characterization, we found that substitution of Fe with Co occurs isoelectronically to form $Ca_{0.5}Bi^{3+}_{0.5}(Fe_{1-x}Co_x)^{3.5+}O_3$ and destabilizes the CD state. This results in materials exhibiting only intermetallic charge transfer behaviour in the region $0.01 < x < 0.67$. The CT transitions for these materials only involves $Fe^{3.5+}$ whereas Co remains in the 3.5+ oxidation state at all temperatures. The doped $Co^{3.5+}$ ions give Pauli-paramagnetic like conducting behavior. The Co-doping effect is very different from that observed in $CaFe_{1-x}Co_xO_3$. The charge transition behavior of $Fe^{3.5+}$ in the present system are also in contrast to those in $Ca_{0.5}Bi_{0.5}FeO_3$ and $Sr_{0.5}Bi_{0.5}FeO_3$.

Introduction

Materials that contain electronic instabilities are exciting because the wide range of routes by which they relieve those instabilities often lead to unusual and/or coupled fundamental properties. The archetypal example material is $CaFeO_3$, which contains iron centres in an electronically unstable +4 oxidation state at 300 K.[1] When cooled below 290 K, the iron disproportionates into an equal mixture of Fe^{3+} and Fe^{5+}. This disproportionation transition is coupled to a structural phase transiton due to the rocksalt ordering of Fe^{3+} and Fe^{5+} and a metal-insulator transition.[1,2] Due to competing interactions between the two types of iron centres, the magnetic structure adopted is a complex incommensurate one.[2] Another way to relieve the electronic instability is via intersite charge transfer (CT) as observed in $LaCu_3Fe_4O_{12}$ where unstable $Fe^{3.75+}$ is reduced to Fe^{3+} by charge transfer from Cu^{2+} ($LaCu^{2+}{}_3Fe^{3.75+}{}_4O_{12} \rightarrow LaCu^{3+}{}_3Fe^{3+}{}_4O_{12}$) below 393 K.[3] This transition is coupled to a structural transition with large volume expansion, a metal-insulator transition, and an antiferromagnetic transition of charge transferred Fe^{3+} spins. A similar CT transition was observed in $BiNiO_3$, where $Bi^{3+}Ni^{3+}O_3$ changes to form $Bi^{3+}_{0.5}Bi^{5+}_{0.5}Ni^{2+}O_3$ under pressure.[4] The Bi ions at the A site of the perovskite structure can be a counter cation for the CT transition.

We recently found $Ca_{0.5}Bi_{0.5}FeO_3$ adopting the perovskite structure (space group *Pnma* Figure 1 (a)) shows sequentially both charge disproportionation (CD) and intersite charge transfer (CT) transitions according to the equation:

$$Ca_{0.5}Bi^{3+}_{0.5}Fe^{3.5+}O_3 \xrightarrow{250\ K} Ca_{0.5}Bi^{3+}_{0.5}Fe^{3+}_{0.67}Fe^{4.5+}_{0.33}O_3 \xrightarrow{200\ K} Ca_{0.5}Bi^{3+}_{0.25}Bi^{5+}_{0.25}Fe^{3+}O_3$$ [5]

In this material, both transitions are accompanied by structural transitions, changes to the transport properties, and magnetic order.[5,6] The CD phase $Ca_{0.5}Bi^{3+}_{0.5}Fe^{3+}_{0.67}Fe^{4.5+}_{0.33}O_3$ shows an unusual layered B-site ordering which results in a magnetic structure in which only the Fe^{3+} centres are magnetically ordered while the $Fe^{4.5+}$ centres remain idle (Figure 1 (b)). On the other hand, the CT phase $Ca_{0.5}Bi^{3+}_{0.25}Bi^{5+}_{0.25}Fe^{3+}O_3$ shows G-type magnetic ordering similar to the orthoferrites with general formula $RFeO_3$ (R = lanthanide or Y; Figure 1 (c)).[6]

In this study we are interested in exploring the cobalt-substituted $Ca_{0.5}Bi_{0.5}Fe_{1-x}Co_xO_3$ materials. In $CaFeO_3$, the partial substitution of Fe for Co up to 50% results in a change in the electronic structure and charge disproportionation behaviour. Charge order melting is first observed up to 10% Co substitution (i.e $CaFe_{0.9}Co_{0.1}O_3$) along with a decrease in the magnetic transition temperature (T_N) with increasing Co content. Between 20 and 50% Co content, the magnetic behaviour changes to ferromagnetic order.[7] The present experimental results on $Ca_{0.5}Bi_{0.5}Fe_{1-x}Co_xO_3$ are compared to those of Co-doped $CaFeO_3$, and the effects of Co-doping to the unusual electronic behaviour exhibited by the parent $x = 0$ material are discussed.

Experimental

Polycrystalline samples of $Ca_{0.5}Bi_{0.5}Fe_{1-x}Co_xO_3$ (x = 0.01, 0.03, 0.05, 0.25, 0.5, 0.67, 0.75, 1) were

synthesised using high temperature high pressure techniques. In order to ensure sample homogeneity, citrate gel precursors were used. Suitable stoichiometric amounts of $CaCO_3$, Bi_2O_3, Fe, and Co powders were dissolved in a minimal quantity of 6 M nitric acid. 1.5 mol equivalents of citric acid and 5 ml of ethylene glycol were added and the solution was heated with constant stirring. Following dehydration of the resulting gels, these were ground into fine powders, placed in alumina crucibles, and heated at 1 °C min^{-1} to 850 °C for 12 hours. The precursor powders were then sealed in Au capsules with an excess of $KClO_4$ as an in-situ oxygen source and heated to 1100°C for 30 mins under a pressure of 6 GPa ($x < 0.67$) or 8 GPa ($x \geq 0.67$) using a DIA cubic anvil press followed by quenching to room temperature. The pressure was slowly released following cooling and the sample washed with distilled water to remove KCl and unreacted $KClO_4$. Additional details regarding the synthesis of large samples suitable for the collection of neutron powder diffraction data are given in the supporting information.

Crystal and magnetic structures were analysed using X-ray and neutron powder diffraction data. Laboratory X-ray powder diffraction data were collected using a Bruker D8 diffractometer using Cu Kα radiation. Synchrotron X-ray powder diffraction data were collected from samples contained within 0.1 mm quartz capillaries using the BL02B2 beamline at Spring-8, Japan and the TPS-09A beamline at NSRRC, Taiwan. Neutron powder diffraction data were collected using the POLARIS diffractometer at ISIS Neutron Source, United Kingdom, from samples contained within a vanadium can. Rietveld refinements were performed using the GSAS program.[8]

Magnetic properties were measured with a commercial Quantum Design MPMS superconducting quantum interference device magnetometer using a field of 100 Oe unless otherwise specified. Mössbauer spectroscopy measurements were carried out to determine the valence and magnetic state of Fe in transmission geometry with a constant-acceleration spectrometer using a $^{57}Co/Rh$ radiation source and were fitted with Lorentzian functions.

Results

Solid Solution and charge states at 300 K

Laboratory X-ray powder diffraction data confirmed the successful synthesis of the entire $Ca_{0.5}Bi_{0.5}Fe_{1-x}Co_xO_3$ (x = 0.01, 0.03, 0.05, 0.25, 0.5, 0.67, 0.75, 1) solid solution. Attempts to prepare the Co-rich members (with $x \geq 0.67$) were not successful at the same conditions previously employed for the synthesis of $Ca_{0.5}Bi_{0.5}FeO_3$ (6 GPa and 1100 °C).[5] A higher pressure of 8 GPa was required to yield these materials.

Synchrotron X-ray powder diffraction data collected at 300 K from $Ca_{0.5}Bi_{0.5}Fe_{1-x}Co_xO_3$ could all be readily indexed on the basis of orthorhombic unit cells (space group *Pmna*) with lattice parameters similar to those of $Ca_{0.5}Bi_{0.5}FeO_3$. Refined lattice parameters at 300 K show a linear variation with composition indicating that this solid solution obeys Vegard's Law (Supporting Information). Rietveld refinement against synchrotron X-ray and neutron powder diffraction data confirmed that the entire

solid solution crystallises in the perovskite structure shown in Figure 1 (a). The resulting fit to the end member $Ca_{0.5}Bi_{0.5}CoO_3$ and the refined structural parameters are given in the supporting information. Neutron powder diffraction data collected at room temperature from the whole solid solution range did not contain any additional features indicating magnetic order. Refinement of the oxygen site occupancy confirmed stoichiometric $Ca_{0.5}Bi_{0.5}Fe_{1-x}Co_xO_3$ compositions.

Mössbauer spectroscopy data collected from $Ca_{0.5}Bi_{0.5}Fe_{0.75}Co_{0.25}O_3$, $Ca_{0.5}Bi_{0.5}Fe_{0.50}Co_{0.50}O_3$, and $Ca_{0.5}Bi_{0.5}Fe_{0.25}Co_{0.75}O_3$ at 300 K could all be fitted with single components with isomer shifts 0.23, 0.24, and 0.28 mm s^{-1} respectively. These values are a good match for $Fe^{3.5+}$ as observed in $Ca_{0.5}Bi_{0.5}FeO_3$ (IS = 0.23 mm s^{-1}, c.f. $Fe^{3+} \sim 0.45$ and $Fe^{4+} \sim 0$)[REF] confirming the presence of unusually high-valent $Fe^{3.5+}$ in these phases.[5]

$Ca_{0.5}Bi_{0.5}Fe_{0.99}Co_{0.01}O_3$

Synchrotron X-ray powder diffraction data collected from $Ca_{0.5}Bi_{0.5}Fe_{0.99}Co_{0.01}O_3$ as a function of temperature are shown in Figure 2 (a) and a plot of the refined lattice parameters as a function of temperature are shown in Figure 3 (a). Magnetisation data collected as a function of temperature is shown in Figure 3 (b). These are very similar to the analogous data collected from $Ca_{0.5}Bi_{0.5}FeO_3$.[5,6] The discontinuities in the variation of lattice parameters with temperature and the features observed in the magnetisation data indicate analogous behaviour consisting of charge disproportionation at approximately 240 K followed by intersite charge transfer at approximately 200 K. Neutron powder diffraction data collected at 300 K, 230 K, and 4.2 K are shown in the supporting information and consistent with this assignment. Additionally, the CD and CT phases of $Ca_{0.5}Bi_{0.5}Fe_{0.99}Co_{0.01}O_3$ adopt the same magnetic structures as the undoped parent phase with refined moments of 2.80(1) μ_B (CD phase at 230 K) and 3.72(1) μ_B (CT phase at 4.2 K) per B-site respectively.

In unsubstituted $Ca_{0.5}Bi_{0.5}FeO_3$, the CD and CT phases coexist at all temperatures below 200 K.[5] The introduction of cobalt appears to destabilise the CD phase and consequently neutron powder diffraction data collected at 4.2 K is well accounted for using only contributions from the CT phase (Supporting Information).

$Ca_{0.5}Bi_{0.5}Fe_{1-x}Co_xO_3$ ($0.03 \leq x < 0.67$)

Synchrotron X-ray powder diffraction data collected from $Ca_{0.5}Bi_{0.5}Fe_{0.97}Co_{0.03}O_3$ as a function of temperature are shown in Figure 2 (b). Only a single phase transition is observed in the variation of lattice parameters as a function of temperature (Figure 2 (b) and Figure 4 (a)). Between 225 K and 160 K two phases are required to correctly account for the data. Similar behaviour is observed for the other members of the $Ca_{0.5}Bi_{0.5}Fe_{1-x}Co_xO_3$ ($0.03 < x < 0.67$) solid solution: a plot of the refined lattice parameters as a function of temperature showed a single discontinuity at approximately 220 K irrespective of composition (Supporting Information).

Bond valence sum calculations using the parameters provided by Brese and O'Keefe from the refined structures of the two phases of $Ca_{0.5}Bi_{0.5}Fe_{0.97}Co_{0.03}O_3$ at 200 K are shown in Table 1.[9] These clearly

show that the average valence of the A-site in the phase that emerges at low temperatures is greater than that of the high temperature phase, while the valence of the iron centers decreases from 3.40 to 3.05. The phase present at low temperatures also shows a significant increase in volume when compared to the high-temperature phase (227.60(1) Å^3 and 230.04(2) Å^3 for the high and low temperature phases respectively at 200 K). This behaviour is consistent with intersite charge transfer behaviour as observed in $Ca_{0.5}Bi_{0.5}FeO_3$. This suggests that the single transition observed in these materials is a charge transfer transition. Data collected from $Ca_{0.5}Bi_{0.5}Fe_{0.97}Co_{0.03}O_3$ below ~ 160 K can be well fitted using only a single phase, indicating complete conversion of the HT phase into the CT phase (Supporting Information).

For all $Ca_{0.5}Bi_{0.5}Fe_{1-x}Co_xO_3$ ($0.03 \leq x < 0.67$) materials, the volume difference between the high-temperature and CT phases decreases with increasing cobalt doping level . For materials $x < 0.25$, the unit cell at 4.2 K is larger than at 300 K, whereas for $x > 0.25$ the low temperature unit cell is smaller than at 300 K despite the phase transition. For $x = 0.25$, the unit cells at 4.2 K and 300 K are the same volume within error (225.02(3) Å^3 and 225.04(6) Å^3 at 4.2 K and 300 K respectively).

Magnetisation data collected from the $x = 0.03$ material as a function of temperature are shown in Figure 4 (b). These show a divergence between zero-field cooled and field cooled data below 240 K with a large increase in the magnetisation that plateaus at 150 K. Overlaying the refined weight fraction of the CT phase shows good agreement with the data in Figure 4 (b). This suggests that, as in $Ca_{0.5}Bi_{0.5}FeO_3$, the magnetic ordering temperature of the CT phase is higher than the phase transition temperature and the structural phase transition is couple to magnetic ordering.[6] Magnetisation data collected from $Ca_{0.5}Bi_{0.5}Fe_{0.75}Co_{0.25}O_3$, and $Ca_{0.5}Bi_{0.5}Fe_{0.50}Co_{0.50}O_3$ are shown in Figure 5 (a) and (b). Neutron powder diffraction data collected from $Ca_{0.5}Bi_{0.5}Fe_{0.97}Co_{0.03}O_3$, $Ca_{0.5}Bi_{0.5}Fe_{0.75}Co_{0.25}O_3$, and $Ca_{0.5}Bi_{0.5}Fe_{0.50}Co_{0.50}O_3$ at 4.2 K show additional features compared to analogous data collected at 300 K (Supporting Information). These additional features are well accounted for using G-type magnetic ordering as in the CT phase of $Ca_{0.5}Bi_{0.5}FeO_3$ with refined moments of 3.70(2) μ_B, 2.76 (2) μ_B, and 1.11(2) μ_B per magnetic center for each phase (Figure 1 (c)).[6]

$Ca_{0.5}Bi_{0.5}Fe_{1-x}Co_xO_3$ ($0.67 \leq x \leq 1$)

X-ray powder diffraction data collected from $Ca_{0.5}Bi_{0.5}Fe_{1-x}Co_xO_3$ ($0.67 < x \leq 1$) as a function of temperature show only the linear variation with temperature expected and no phase transitions between 100 K and 300 K (Figure 6). For $Ca_{0.5}Bi_{0.5}CoO_3$, observed, calculated, and difference plots of a Rietveld refinement against synchrotron X-ray powder diffraction data, as well as structural information and fit statistics are given in the Supporting Information.

Magnetization data collected from $Ca_{0.5}Bi_{0.5}Fe_{0.25}Co_{0.75}O_3$ show a divergence between ZFC and FC data at approximately 150 K while data collected from $Ca_{0.5}Bi_{0.5}CoO_3$ show nearly temperature-independent small susceptibility with upturn at low temperature (<30 K). Resistivity data collected as a function of temperature are shown in the supporting information and are likewise free of any obvious

transitions. The observed results suggest Pauli-paramagnetic like behavior of $Ca_{0.5}Bi_{0.5}CoO_3$. Neutron powder diffraction data collected from these materials at 4.2 K do not show any additional features compared to equivalent data collected at 300 K, suggesting that the magnetic transition at 150 K is a spin glass freezing transition (Supporting Information).

Discussion

For all $Ca_{0.5}Bi_{0.5}Fe_{1-x}Co_xO_3$ ($0 < x < 1$), Mössbauer spectroscopy data and bond valence sum calculations are consistent with the presence of Bi^{3+} and $Fe^{3.5+}$ at 300 K and, through charge balancing, $Co^{3.5+}$ (i.e. $Ca_{0.5}Bi^{3+}_{0.5}(Fe_{1-x}Co_x)^{3.5+}O_3$). In $Ca_{0.5}Bi_{0.5}CoO_3$, the refined lattice parameters and bond valence sum calculations from the refined structure suggest that at room temperature this material contains Bi^{3+} and $Co^{3.5+}$. In addition, the lack of any structural phase transition or magnetic anomaly in this material suggests that neither CD nor CT behaviour is exhibited and these are the oxidation states at all $T \geq 5$ K. The effect of cobalt substitution can be explained by considering the different behavior of $CaFeO_3$ and $CaCoO_3$.

The two charge transitions in $Ca_{0.5}Bi_{0.5}FeO_3$ respond differently to the substitution of iron for cobalt. The charge disproportionation of unusually high-valent $Fe^{3.5+}$ centers in the parent is remarkably fragile, as any substitution greater than 1 % leads to suppression of the CD behaviour. This is in sharp contrast to the behaviour of Co-substituted $CaFeO_3$, in which charge order melting only occurs at 10 % substitution – an order of magnitude difference.[7] The CT behaviour on the other hand is remarkably tolerant to Co substitution; exhibiting wide tunability all the way to 67 % Co substitution. The lack of CD in $Ca_{0.5}Bi_{0.5}Fe_{1-x}Co_xO_3$ ($x < 0.01$) can be ascribed to a destabilization of the CD state due to broadening of the oxygen hole band as observed in $CaFe_{1-x}Co_xO_3$.[7] The destabilization of the CD state has the additional feature of enabling complete conversion of the high temperature phase to the CT phase. At 5 K, $Ca_{0.5}Bi_{0.5}FeO_3$ exists as a mixture of $Ca_{0.5}Bi^{3+}_{0.5}Fe^{3+}_{0.67}Fe^{5+}_{0.33}O_3$ and $Ca_{0.5}Bi^{3+}_{0.25}Bi^{5+}_{0.25}Fe^{3+}O_3$ whereas $Ca_{0.5}Bi_{0.5}Fe_{0.99}Co_{0.01}O_3$ does not contain any appreciable quantity of the CD phase at 4.2 K.[5,6]

The behavior of the Co-substituted $Ca_{0.5}Bi_{0.5}Fe_{1-x}Co_xO_3$ phases stand in contrast to that of the A-site substituted $Ca_{0.5-x}Sr_xBi_{0.5}FeO_3$ where small amounts of Sr substitution suppress the CT transition and result in a 3:1 ratio of charge disproportionated Fe^{3+} and Fe^{5+} at low temperatures. [10]

For $Ca_{0.5}Bi_{0.5}Fe_{1-x}Co_xO_3$ ($x < 0.67$), both the magnitude of the volume expansion and the ordered moment show linear dependence on the cobalt substitution level. This can be readily explained if only the iron centers are involved in charge transfer. A plot of the refined ordered moment as a function of cobalt content $Ca_{0.5}Bi_{0.5}Fe_{1-x}Co_xO_3$ (x = 0.03, 0.05, 0.25, 0.5, 0.75) is shown in **Error! Reference source not found.** (a). A linear dependence of the moment with Co doping level is observed for $0.03 < x < 0.67$. If $Co^{3.5+}$ is not involved in the CT transition, the linear dependence of the ordered moment and volume changes on Co substitution can be ascribed to a transition of the form:

$$Ca_{0.5}Bi^{3+}_{0.5}(Fe_{1-x}Co_x)^{3.5+}O_3 \rightarrow Ca_{0.5}Bi^{3+}_{(1+x)/4}\,Bi^{5+}_{(1-x)/4}Fe^{3+}_{1-x}Co^{3.5+}_{x}O_3.$$

The observed linear dependence of refined magnetic moment at 4.2 K can be explained by the decrease in concentration of the magnetic Fe^{3+} ions, which are stabilized by charge transfer. The lower refined moment compared to the ideal moment of Fe^{3+} (S = 5/2) is likely due to the strong hybridization with neighboring oxygen. A phase diagram of the electronic states in $Ca_{0.5}Bi_{0.5}Fe_{1-x}Co_xO_3$ ($0 \leq x \leq 1$) as a function of temperature and composition is shown in Figure 6 (b).

The effect of Co substitution on the magnetic behavior is also very different from that for $CaFeO_3$, where more than 20% Co substitution induces ferromagnetic behavior with magnetic transition temperatures at approximately 180-200 K. In $Ca_{0.5}Bi_{0.5}Fe_{1-x}Co_xO_3$, no such behavior is observed indicating that $Co^{3.5+}$ centers do not facilitate ferromagnetic interaction between Fe ions. It should also be noted that $Co^{3.5+}$ in $Ca_{0.5}Bi_{0.5}Fe_{1-x}Co_xO_3$ ($x \geq 0.67$) show Pauli-paramagnetic and conducting behavior. This is likely due to $x \sim 0.67$ being close to the electrical percolation threshold beyond which the conductivity of $Co^{3.5+}$ dominates.

The behavior of the Co-rich members of the solid solution can be contrasted with the properties of other $Co^{3.5+}$-containing compounds. Both rhombohedral $La_{0.5}Ca_{0.5}CoO_3$ and tetragonal $La_{0.5}Ca_{0.5}CoO_3$, for instance, are ferromagnetic metals with ordering temperatures of $T \approx 280$ and 160 K respectively.[11–13] The lack of a magnetic ordering transition in $Ca_{0.5}Bi_{0.5}CoO_3$ is not surprising given the increased octahedral tilt distortions which reduce the orbital overlap (Co-O1-Co = 156.6 ° and Co-O2-Co = 148.6 ° compared with 164.0 ° and 159.5 ° for analogous angles in $La_{0.5}Ca_{0.5}CoO_3$).[12,14]

All materials adopt the perovskite structure and the oxidation state of iron at 300 K is +3.5, but they show dramatic differences in behavior on cooling: $Ca_{0.5}Bi_{0.5}FeO_3$ shows successively charge disproportionation and charge transfer; $Sr_{0.5}Bi_{0.5}FeO_3$ shows only charge disproportionation but does not show charge ordering, while $Ca_{0.5}Bi_{0.5}Fe_{1-x}Co_xO_3$ ($0.03 \leq x < 0.67$) show only charge transfer.[5,10] This highlights the facile tunability of the successive charge transitions in $Ca_{0.5}Bi_{0.5}FeO_3$.

Conclusion

The whole solid solution $Ca_{0.5}Bi_{0.5}Fe_{1-x}Co_xO_3$ ($0 \leq x \leq 1$) has been successfully prepared. Of the two sequential charge transitions present in the $x = 0$ parent material, the higher temperature CD transition is suppressed when $x > 0.01$ while the CT transition is only suppressed when $x \geq 0.67$. For $0.03 < x < 0.67$, the negative thermal expansion and magnetic moments show simple linear dependence on the cobalt content, indicating the facile tunability of the fundamental properties in this series of phases. Unlike $Fe^{3.5+}$, $Co^{3.5+}$ cations in this phase are not susceptible to any charge transition.

Acknowledgements

This work was supported by JSPS Grants-in-Aid for Scientific Research (Grants No. 16H02266, 16H00888, 15F15036, and 17F17039), by a JSPS Core-to-Core program (A) Advanced Research

Networks, by a grant for the Joint Project of Chemical Synthesis Core Research Institutions from MEXT, and by grants from the EPSRC. Support was also provided by the Royal Society. We thank STFC for the provision of ISIS beamtime, and Dr. Ron Smith for assistance with data collection. We also than Drs. We-Tin Chen, Yu-Chun Chuang, and Hwo-Shuenn Sheu in NSRRC in Taiwan for help with synchrotron diffraction data collection.

* denisromero.fabio.3e@kyoto-u.ac.jp (FDR) and shimak@scl.kyoto-u.ac.jp (YS)

References

(1) Takano, M.; Nakanishi, N.; Takeda, Y.; Naka, S.; Takada, T. *Mater. Res. Bull.* **1977**, *12* (9), 923.

(2) Woodward, P. M.; Cox, D. E.; Moshopoulou, E.; Sleight, A. W.; Morimoto, S. *Phys. Rev. B* **2000**, *62* (2), 844.

(3) Long, Y. W.; Hayashi, N.; Saito, T.; Azuma, M.; Muranaka, S.; Shimakawa, Y. *Nature* **2009**, *458* (7234), 60.

(4) Azuma, M.; Carlsson, S.; Rodgers, J.; Tucker, M. G.; Tsujimoto, M.; Ishiwata, S.; Isoda, S.; Shimakawa, Y.; Takano, M.; Attfield, J. P. *J. Am. Chem. Soc.* **2007**, *129* (46), 14433.

(5) Hosaka, Y.; Denis Romero, F.; Ichikawa, N.; Saito, T.; Shimakawa, Y. *Angew. Chemie Int. Ed.* **2017**, *56* (15), 4243.

(6) Denis Romero, F.; Hosaka, Y.; Ichikawa, N.; Saito, T.; McNally, G.; Attfield, J. P.; Shimakawa, Y. *Phys. Rev. B* **2017**, *96* (6), 64434.

(7) Kawasaki, S.; Takano, M.; Kanno, R.; Takeda, T.; Fujimori, A. *J. Phys. Soc. Japan* **1998**, *67* (5), 1529.

(8) Larson, A. C.; Dreele, R. B. Von. *Los Alamos Natl. Lab. Rep. LAUR* **2000**, 86.

(9) Brese, N. E.; O'Keeffe, M. *Acta Crystallogr. Sect. B Struct. Sci.* **1991**, *47* (2), 192.

(10) Xiong, P.; Romero, F. D.; Hosaka, Y.; Guo, H.; Saito, T.; Chen, W.-T.; Chuang, Y.-C.; Sheu, H.-S.; McNally, G.; Attfield, J. P.; Shimakawa, Y. *Inorg. Chem.* **2018**, *57* (2), 843.

(11) Goodenough, J. B. *Mater. Res. Bull.* **1971**, *6* (10), 967.

(12) Golosova, N. O.; Kozlenko, D. P.; Lukin, E. V.; Savenko, B. N. *JETP Lett.* **2010**, *92* (2), 110.

(13) Masuda, H.; Fujita, T.; Miyashita, T.; Soda, M.; Yasui, Y.; Kobayashi, Y.; Sato, M. *J. Phys. Soc. Japan* **2003**, *72* (4), 873.

(14) Goodenough, J. B. *Magnetism and the chemical bond*; Interscience monographs on chemistry: Inorganic chemistry section; Interscience Publishers, 1963.

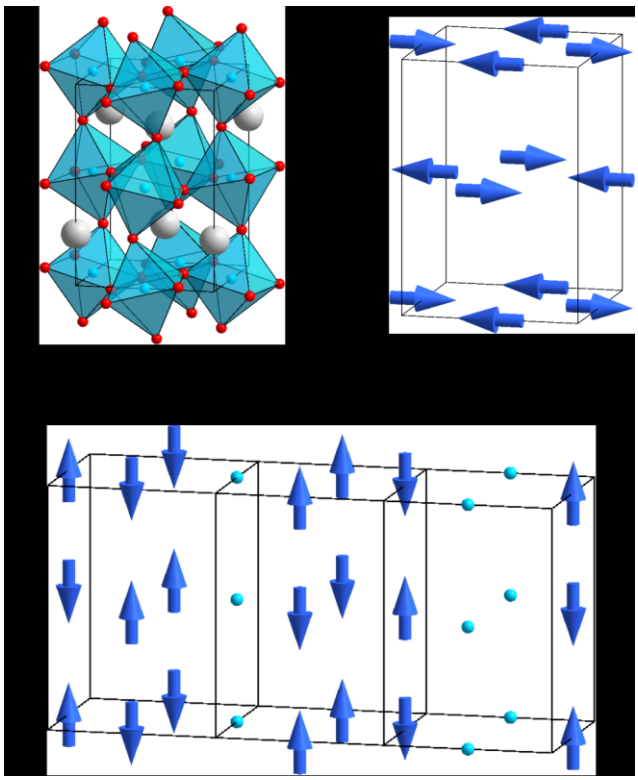

Figure 1: (a) Crystal structure of $Ca_{0.5}Bi_{0.5}Fe_{1-x}Co_xO_3$. (b) Magnetic structure of the CD phases (k = 0, 0, 1/3). (c) G-type antiferromagnetic structure of the CT phases (k = 0, 0, 0).

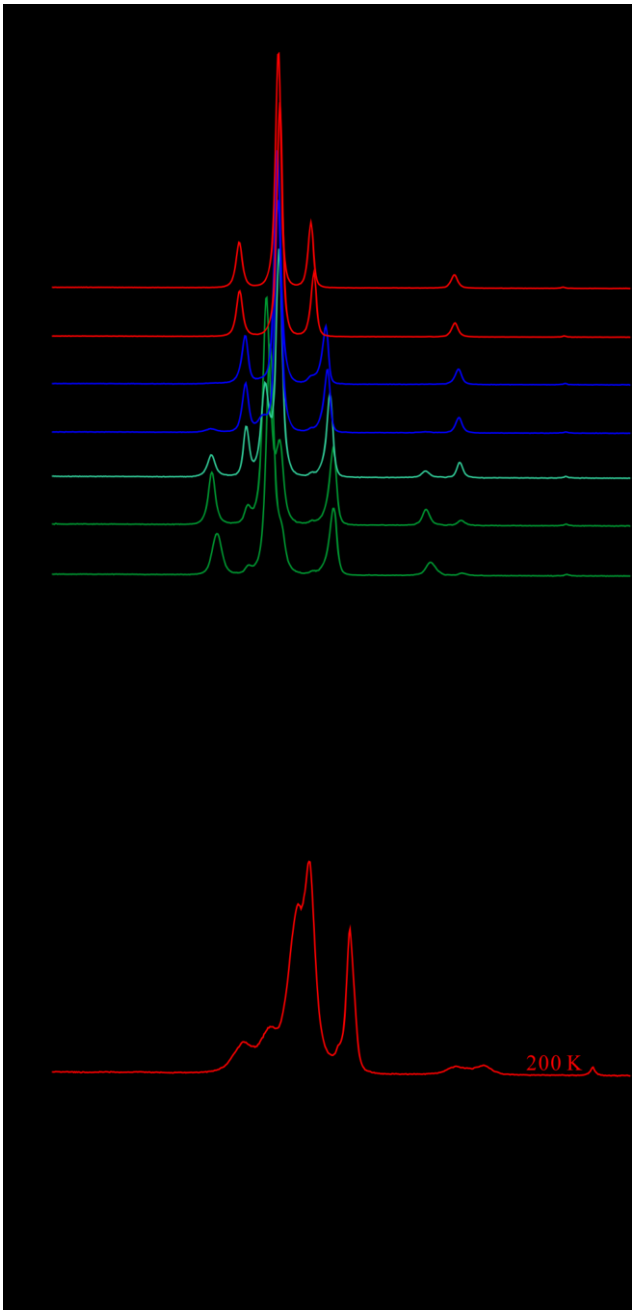

Figure 2: Synchrotron X-ray diffraction data collected as a function of temperature from: (a) $Ca_{0.5}Bi_{0.5}Fe_{0.99}Co_{0.01}O_3$ and (b) $Ca_{0.5}Bi_{0.5}Fe_{0.97}Co_{0.03}O_3$. In (a) the three different colours correspond to regions where the majority phase is the HT phase (red), CD phase (blue) and CT phase (green). In (b) the highlighted data at 200 K clearly shows the two-phase behaviour in the intermediate temperature regime.

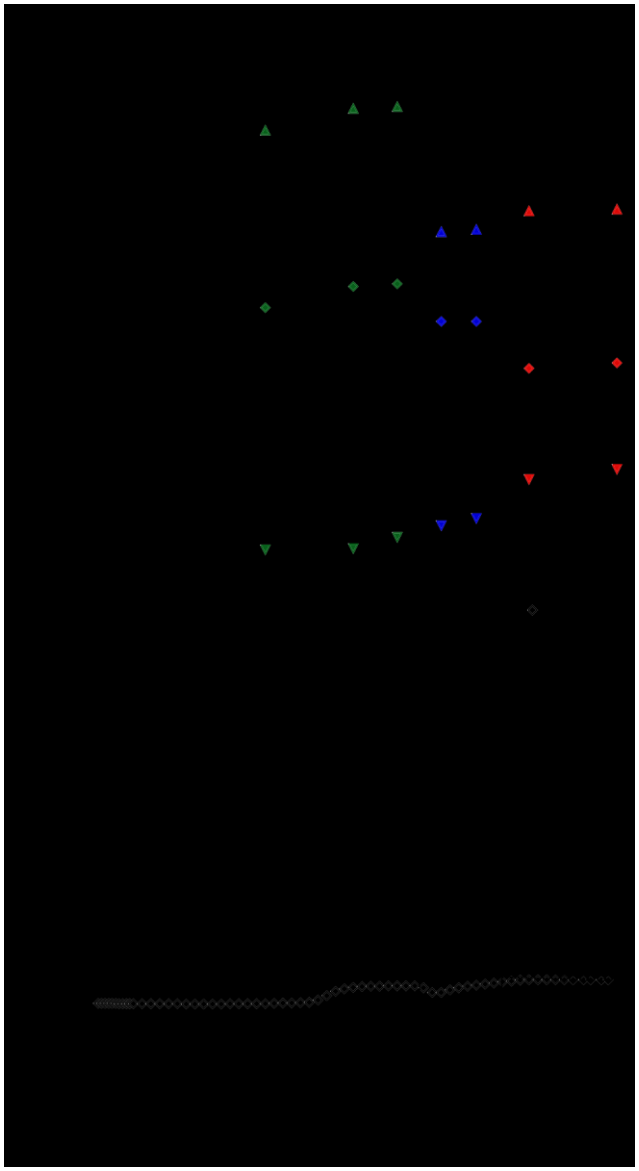

Figure 3: (a) Lattice parameters of the majority phase of $Ca_{0.5}Bi_{0.5}Fe_{0.99}Co_{0.01}O_3$ refined against synchrotron X-ray powder diffraction data as a function of temperature. (b) Magnetization data collected from $Ca_{0.5}Bi_{0.5}Fe_{0.99}Co_{0.01}O_3$ as a function of temperature.

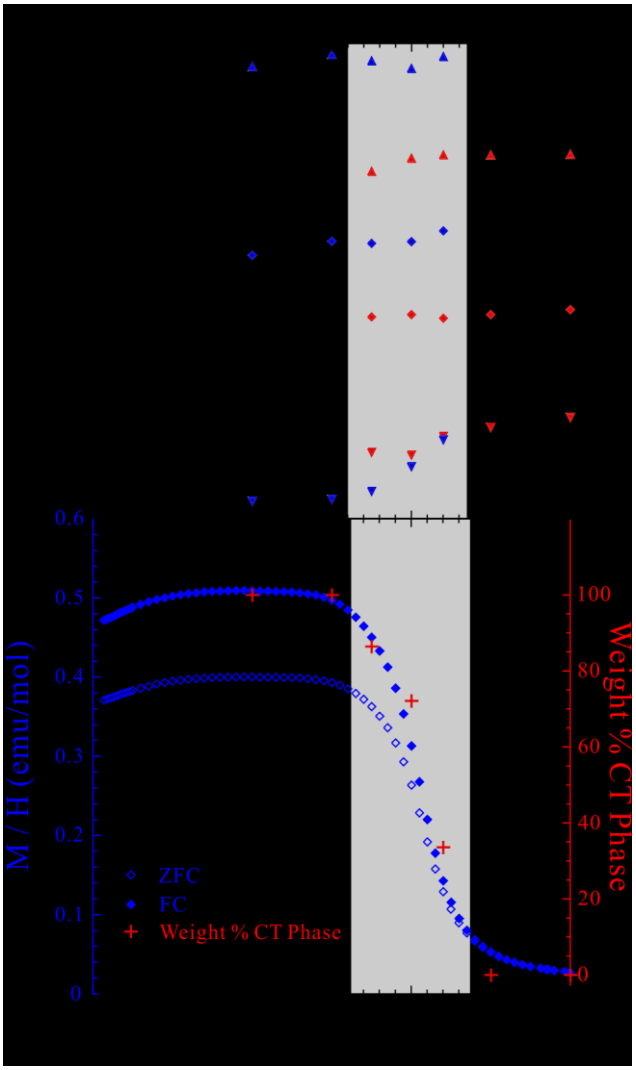

Figure 4: (a) Lattice parameters of $Ca_{0.5}Bi_{0.5}Fe_{0.97}Co_{0.03}O_3$ refined against synchrotron X-ray powder diffraction data as a function of temperature. Red markers correspond to the high temperature high-valent Fe phase while the blue markers correspond to contributions from the low temperature CT phase. For data collected in the shaded region, a mixture of both phases is required to correctly account for the data. (b) Magnetization data collected from $Ca_{0.5}Bi_{0.5}Fe_{0.97}Co_{0.03}O_3$ as a function of temperature (blue) and refined weight percentage of the CT phase against synchrotron X-ray powder diffraction data (red).

	Ca^{2+} $R_{ij} = 1.967$	Bi^{3+} $R_{ij} = 2.09$	Fe^{3+} $R_{ij} = 1.759$	Co^{3+} $R_{ij} = 1.70$
HT Phase	2.10	2.92	3.40	2.90
CT Phase	2.52	3.51	3.05	2.60

Table 1: Bond valence sums calculated from the two phases of $Ca_{0.5}Bi_{0.5}Fe_{0.97}Co_{0.03}O_3$ at 200 K refined against synchrotron X-ray powder diffraction data.

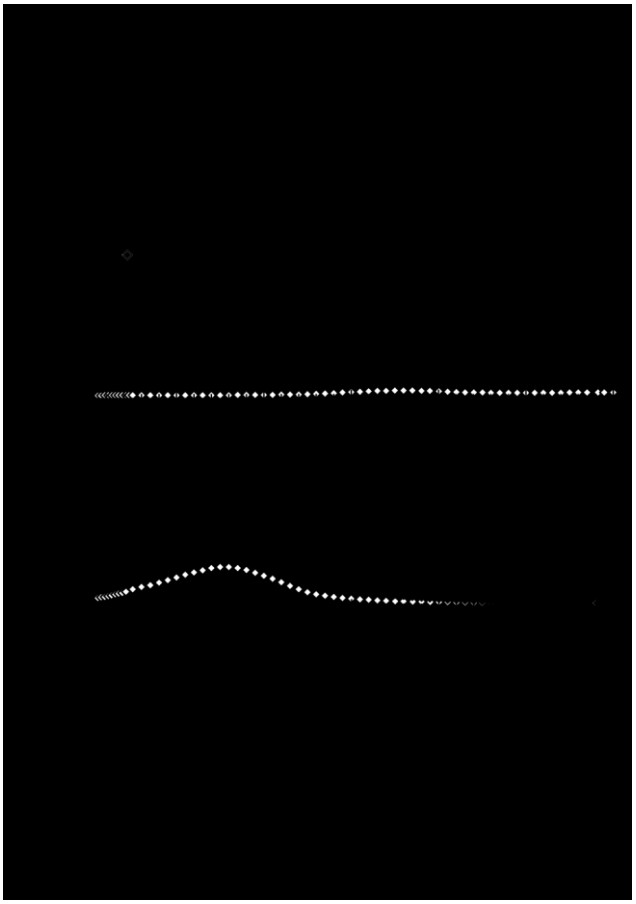

Figure 5: Magnetization data collected from (a) $Ca_{0.5}Bi_{0.5}Fe_{0.75}Co_{0.25}O_3$, (b) $Ca_{0.5}Bi_{0.5}Fe_{0.5}Co_{0.5}O_3$, and (c) $Ca_{0.5}Bi_{0.5}Fe_{0.25}Co_{0.75}O_3$ as a function of temperature.

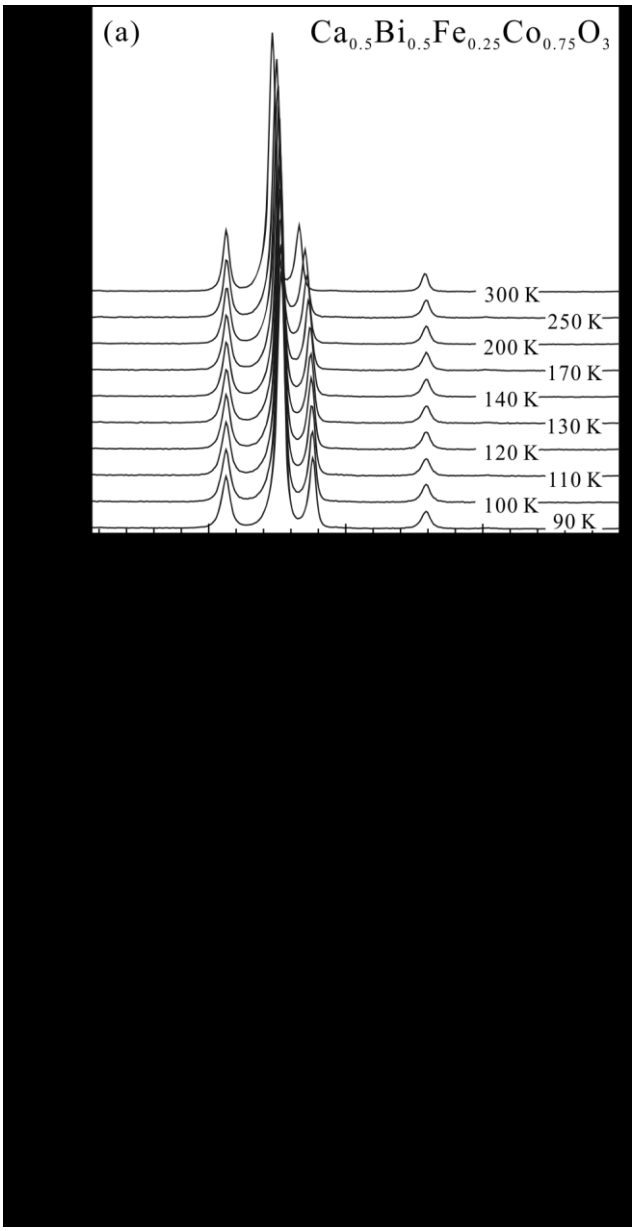

Figure 6: (a) Synchrotron X-ray powder diffraction data collected from $Ca_{0.5}Bi_{0.5}Fe_{0.25}Co_{0.75}O_3$ at various temperatures. (b) Lattice parameters of $Ca_{0.5}Bi_{0.5}Fe_{0.25}Co_{0.75}O_3$ refined against synchrotron X-ray powder diffraction data as a function of temperature.

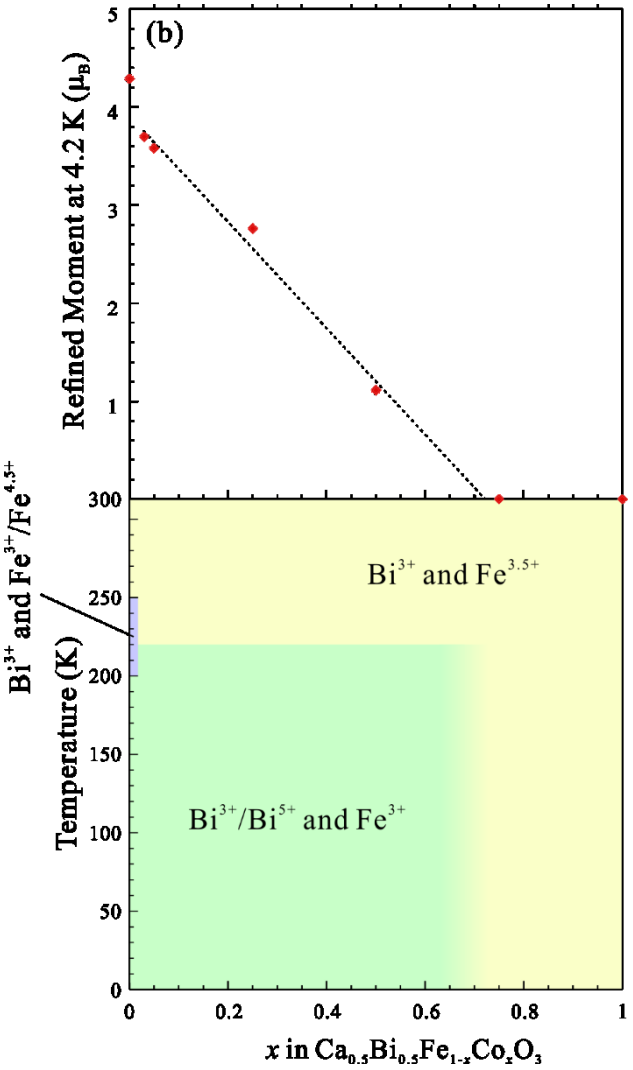

Figure 7: (a) The refined ordered magnetic moment at 4.2 K as a function of x. (b) Electronic phase diagram of $Ca_{0.5}Bi_{0.5}Fe_{1-x}Co_xO_3$ ($0 \leq x \leq 1$) as a function of composition and temperature.